arXiv:1407.3396v1 [cond-mat.soft] 12 Jul 2014

Stripe formation in horizontally oscillating granular suspensions

Robabeh Moosavi,[1] Maniya Maleki,[1,*] M. Reza Shaebani,[2,†] J. C. Ruiz-Suárez,[3] and Eric Clément[4]

[1]*Department of Physics, Institute for Advanced Studies in Basic Sciences, Zanjan 45137-66731, Iran*
[2]*Department of Theoretical Physics, Saarland University, D-66041 Saarbrücken, Germany*
[3]*CINVESTAV-Monterrey, PIIT, Apodaca, Nuevo Leon, 66600, Mexico*
[4]*PMMH, ESPCI, UMR CNRS 7636 and Université Paris 6 et Paris 7, 75005 Paris, France*

(Dated: July 15, 2014)

We present the results of an experimental study of pattern formation in horizontally oscillating granular suspensions. Starting from a homogeneous state, the suspension turns into a striped pattern within a specific range of frequencies and amplitudes of oscillation. We observe an initial development of layered structures perpendicular to the vibration direction and a gradual coarsening of the stripes. However, both processes gradually slow down and eventually saturate. The probability distribution of the stripe width $P(w)$ approaches a nonmonotonic steady-state form which can be approximated by a Poisson distribution. We observe similar structures in MD simulations of soft spherical particles coupled to the motion of the surrounding fluid.

PACS numbers: 45.70.Qj, 45.70.Mg, 47.54.-r

I. INTRODUCTION

Granular mixtures and suspensions exhibit a rich variety of behavior, including segregation, clustering, and pattern formation, when subjected to mechanical agitation [1, 2]. Because of the ubiquity of such phenomena in nature and industry, understanding the mechanisms behind the instability of homogeneous state in granular systems is of great interest within the physics and engineering communities. When a mixture of dry grains, differing in shape, size, density, or other physical properties is agitated, separation between different species may occur depending on the properties of the external drive. In the case of strong driving the dynamics is dominated by inelastic binary collisions. Here, effective long-range interactions appear between the particles of the same type due to the presence of hydrodynamic fluctuations [3, 4], leading to a variety of collective behaviors. With decreasing the driving strength, durable contacts form between the particles, eventually becoming dominant. In this regime, friction plays a crucial role [5, 6] and relevant separation mechanisms are e.g. local rearrangements, percolation, and convection [7]. The dynamics is more complex in granular suspensions due to the influence of the fluid on the particles, causing e.g. anisotropic hydrodynamic forces or viscous drag. The existence of underlying hydrodynamic interactions is the reason behind different time scales for pattern formation in suspensions compared with dry mixtures.

The observed behavior also depends on the agitating method by which energy is injected into the system. For example, vertical vibrations have attracted a lot of attention since they can lead to variants of the Brazil nut effect [8, 9] or clustering [3, 10]. The dynamics of horizontally driven systems is even more diverse. Shear-induced segregation has been reported in suspensions [11] and granular mixtures in a split-bottom cell [12], where the presence of shear bands [13] renders the system inhomogeneous. Horizontal swirling motion may also lead to separation of different species [14]. One of the most interesting types of instability is the formation of stripes, which has been observed in horizontal shaking or oscillatory excitation of binary mixtures of dry particles [15–23], or a single type of dry particles with a moderate size polydispersity [6]. There have been less studies on pattern formation in suspensions. Sánchez et al. [24] investigated the emerging striped patterns in a fluid-immersed mixture of bronze and glass spheres subjected to horizontal vibration, and proposed a mechanism for the formation of stripes based on the differential influence of drag on the components of the mixture. However, the development of chain-like structures has been observed even between identical spheres in oscillatory fluid flows in MD simulations [25].

In this Letter, we study the formation of stripes in a suspension consisting of a single type of particles im-

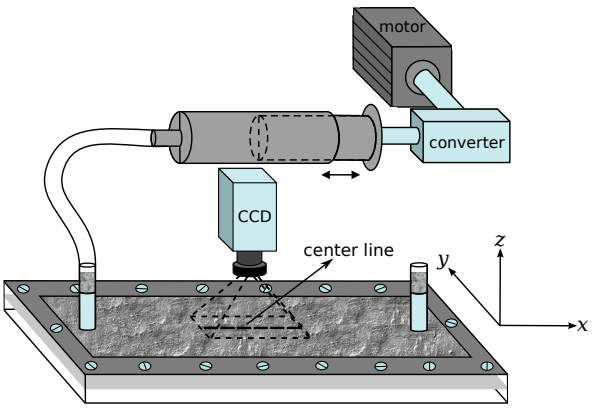

FIG. 1: Schematic picture of the experimental setup.

*Electronic address: m˙maleki@iasbs.ac.ir
†Electronic address: shaebani@lusi.uni-sb.de

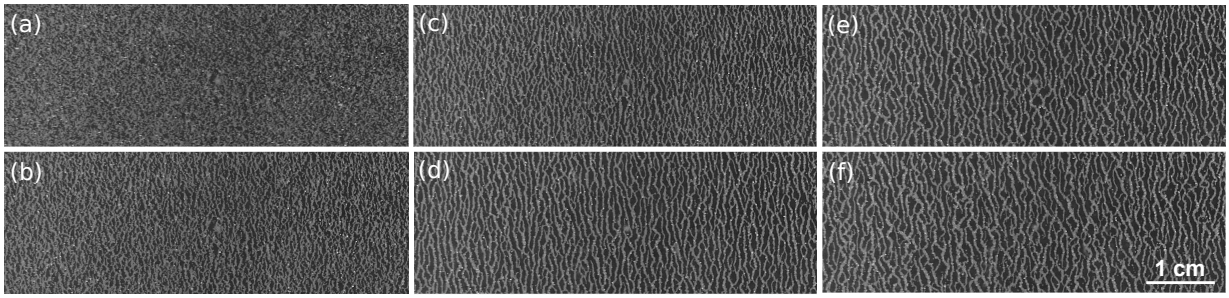

FIG. 2: Evolution of the stripe patterns in a suspension of polystyrene beads (bright) immersed in a NaCl aqueous solution (dark), which is vibrated at f=19.8 Hz and amplitude of vibration A=0.21 mm. Snapshots are taken at t=4, 12, 20, 52, 104 and 340 seconds, from (a) to (f), respectively.

mersed in water, which is subjected to horizontal sinusoidal vibration. We elucidate how the striped pattern evolves in time by considering the structure at the particle level. The focus of research so far has been on identifying the criteria under which the stripes emerge. It is known that no pattern forms at extremely low or high frequencies and amplitudes of vibration [6, 23, 24] or below a certain level of the density of particles [21–23]. On the other hand, within the appropriate range of parameters, stripe formation is a remarkably dominant process. For example, even initially separated phases exhibit shear-induced instabilities under oscillatory excitation [16, 20, 26] and ultimately end up with stripe-like structures. However, the structural properties of the patterns and their spatial and temporal evolution is poorly investigated and understood. It has been shown that a gradual coarsening of the structure occurs [17, 21–24, 27], and that the average width of the stripes increases with increasing the particle density [21–23]. Here, we characterize the structure by measuring the thickness w of the stripes. By monitoring the time evolution of the stripe-width probability distribution $P(w)$ at a given particle density, we verify that the coarsening procedure finally stops and $P(w)$ tends towards a steady state nonmonotonic distribution with a peak around 3 particle-diameter thickness. Besides coarsening, our results evidence the existence of another underlying dynamical process, which simultaneously arranges the particles in vertical layers oriented in the vibration direction. MD simulations of intruder particles immersed in a viscous fluid reproduces the experimentally observed patterns.

II. EXPERIMENTAL SETUP

Our experimental setup is a Hele-Shaw cell consisting of two parallel plexiglass plates of lateral sizes 20cm×5cm separated by a distance s=400 μm. The gap s is accurately controlled by using a Teflon sealed Mylar sheet which is sandwiched between the plates along the perimeter of the cell by small screws. A schematic picture of the setup is shown in Fig. 1. The cell is filled with a suspension which contains either polystyrene or glass beads immersed in water. Although similar patterns form in both cases, here we only present the results of the polystyrene suspension. The beads are spherical with diameter d=80 μm and density ρ=1.05 g/cm^3 and occupy a volume fraction of 7%. To avoid electrostatic effects, we use a NaCl aqueous solution with a density of ρ_s=1.101 g/cm^3.

Two inlet and outlet holes are created in the top plate close to the two ends of the cell along the x direction (see Fig. 1). The outlet hole is exposed to the open air, and the inlet hole is connected to a syringe by means of a soft silicone tube. The syringe is attached to a mechanical converter which transforms the rotational motion of an AC motor into a sinusoidal vibration. This periodic motion is transferred to the syringe and induces a back and forth motion of the suspension inside the tube and cell. This is a novel method to produce oscillatory motion by vibrating the suspension itself instead of the container. The frequency of the vibrations is controlled by an AC speed controller, and the amplitude is held constant at A=0.21 mm. The cell is filled with suspension, without allowing visible air bubbles to be trapped inside.

We image the suspension from above with a CCD camera with a resolution of 40 μm/pixel. The resulting images are indeed the projections of particle configurations into the $x-y$ plane. The camera zooms in on a region of size 6cm×2cm around the center of the cell (see Fig. 1), where the flow field remains uniform far from the boundaries. In order to characterize the structural properties of the patterns, the images can be rather easily analyzed since the contrast between the solution and the grains gives an opportunity to clearly distinguish between them. Thus a simple thresholding converts the gray-scale images into binary ones, with 1 (white) and 0 (black) pixels denoting the grains and the solution, respectively.

III. FORMATION OF STRIPES

Starting from a well-mixed initial condition (with density fluctuations below 5% on grids of one hundred particle-diameter size), the homogeneous state becomes unstable within the first few seconds, and stripe patterns

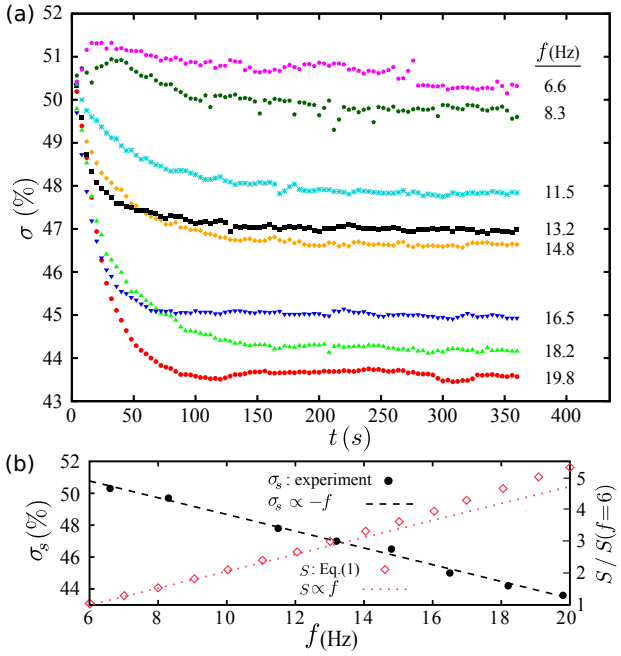

FIG. 3: (a) The area fraction σ occupied by grains as a function of time for a suspension vibrated with amplitude A=0.21 mm at different frequencies f. (b) The stationary value of the occupied area fraction σ_s and the average Shields parameter S versus the vibration frequency f.

emerge which span the entire area of the cell. Clear stripe formation is observed within the moderate frequency range of 6−20 Hz, while no pattern forms below a volume fraction of 4% or above 15% . However, we do not aim here at exploring the frequency-amplitude space for the pattern formation subdomain. Figure 2 shows the time development of the system under horizontal sinusoidal vibration at frequency f=19.8 Hz. The stripes form nearly perpendicular to the oscillation direction and exhibit a branched structure with a persistence length of a few millimeters (i.e. a few tens of particle diameters). A closer look at the evolution of the system interestingly indicates the presence of two underlying dynamical processes: (i) development of layered structures, and (ii) coarsening. The freely floating particles and/or the randomly formed stripes organize themselves into layers along the vertical axis perpendicular to the vibration direction on one hand, and merge into thicker horizontal bands on the other hand.

Let us first investigate the ordering of particles in layers. If the particles sit on top of each other along the z direction, they should occupy a smaller area fraction of the cell when observed from the top view. Note that the thickness of the cell allows the formation of layers with heights of up to 5 particle diameters. We measure the occupied area fraction σ (i.e. the ratio between the number of white pixels and the total number of pixels in a picture) during the experiment for several values of the oscillation frequency. While σ remains unchanged or quickly (in a few seconds) reaches a steady value at low frequencies, it initially decreases with time for high frequencies. The results shown in Fig. 3(a) however reveal that the slope gradually decreases, and σ eventually saturates towards a stationary value σ_s over a characteristic time τ_l. We observe no clear dependence of τ_l on f, but the saturation value σ_s approximately linearly decreases with increasing f [see Fig. 3(b)], indicating that the ordering of particles in layers is more pronounced at higher frequencies. A plausible scenario is that a higher f induces a stronger shear stress τ ($\sim\partial v/\partial z$) which increases the resuspension of sedimenting particles (reflected in the increase of the Shields parameter $S\sim\tau$) and, thus, enhances the layering effect. To estimate $S(f)$, we solve Navier-Stokes and continuity equations for the fluid flow between two infinite parallel plates (i.e. far from the boundaries in the $x-y$ plane), leading to the diffusion equation $\frac{\partial v_x}{\partial t}=\nu\frac{\partial^2 v_x}{\partial z^2}$, with ν being the kinematic viscosity. The solution should fulfill the boundary conditions $v_x(z=0,t)=v_x(z=L_z,t)=0$ and $v_x(z=\frac{L_z}{2},t)=A\omega\cos(\omega t)$. For simplicity, we take the solution in the limit of $\sqrt{2\nu/\omega}\ll L_z$ and obtain the average Shields parameter over one period of oscillation and an arbitrary sediment layer Δ as

$$S(f)\sim\frac{1}{\Delta}\int_0^{\Delta} f\int_0^{\frac{1}{f}}\left|\frac{\partial v(z,t)}{\partial z}\right|\mathrm{d}t\,\mathrm{d}z=\frac{2\pi f}{\Delta}\left(1-e^{-\Delta\sqrt{\frac{\pi f}{\nu}}}\right). \quad (1)$$

As shown in Fig. 3(b), S grows slightly faster than linear with f (with an exponent $1<\alpha<3/2$), which leads to a more pronounced ordering of particles in layers.

Next, we address the coarsening behavior. Figure 2 shows that the stripes gradually coarsen, i.e. thin stripes merge and form thicker ones. However, the stripes may also shrink, dissolve, or even branch to smaller stripes. The competition eventually leads to a dynamical saturation where the overall shape of the pattern becomes time invariant. Coarsening has been reported for dry [17, 21–23] or fluid-immersed [24] binary mixtures of grains. The process is more clearly visualized in Fig. 4, where the time evolution of a specific part of the cell is displayed. To this aim, we focused on an imaginary line segment around the middle of the cell oriented along the vibration direction ("center-line" in Fig. 1). This line intersects many stripes which evolve in time. By recording a time-lapse sequence of frames over a few minutes, it is shown in Fig. 4 that

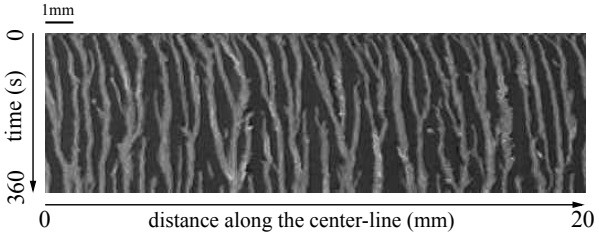

FIG. 4: Time-lapse image of the patterns formed along the center-line of the cell, at the same parameter values as in Fig. 2.

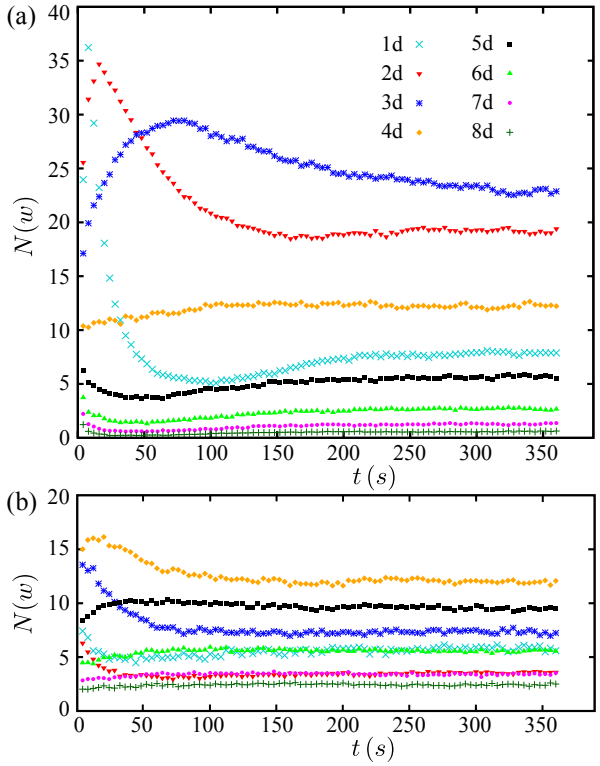

FIG. 5: The average width-resolved number of stripes $N(w)$ along the x-axis versus time, at frequency (a) f=19.8 Hz and (b) f=6.6 Hz. The results are separately shown for several values of w, denoted in the units of grain diameter d.

the mean number of stripes along the center-line initially decreases while their thicknesses grow on average. However, a steady state is reached after a characteristic time τ_c.

We would like to emphasize that the nature of layering and coarsening processes are different, thus, they develop on different time scales. For example, one obtains $\tau_l \sim 100$ s vs. $\tau_c \sim 200$ s at frequency f=19.8 Hz. Moreover, the layering mechanism is fully suppressed in a quasi two-dimensional system, while the coarsening continues to occur. Another point is that both processes reach a dynamical saturation, meaning that the stripes continuously form, merge, or dissolve in time, even at $t > \tau_l, \tau_c$, only the relevant statistical measures, like the occupied area fraction σ or the average stripe thickness, remain almost unchanged.

In order to quantitatively describe the coarsening procedure we categorize the stripes in terms of their width w (by rounding off w/d to integer numbers), and determine the number of stripes $N(w)$ in each category. This is done for each frame by scanning through each of the few hundreds of horizontal lines along the oscillation direction. In Fig. 5(a) we show the time evolution of $N(w)$ for several values of thickness w at high frequency f=19.8 Hz. Interestingly, it turns out that N evolves differently in time for different values of w. Apart from an initial transient, $N(w)$ decreases rather fast for thin

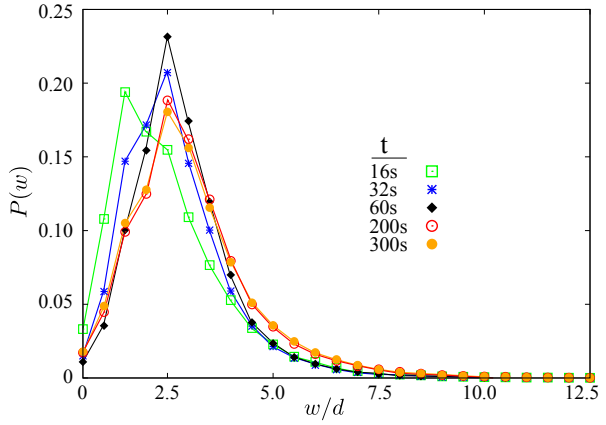

FIG. 6: Evolution of the probability distribution of the stripe width $P(w)$, obtained from experiments at f=19.8 Hz.

stripes ($w/d \simeq 1, 2$) while it considerably increases with time for intermediate values of thickness ($w/d \simeq 3$) with a peak value around $t \sim 70$ s. Comparison with thick stripes reveals only very modest changes in $N(w)$ for $w/d \geq 4$. Moreover, the curves asymptotically converge to different values with a noticeable nonmonotonic ordering so that the stripes of width $w_{\max} \sim 3d$ are the most frequent ones at long times.

A comparison between the results at high and low values of f reveals that the behavior also depends on the vibration frequency. In Fig. 5(b) we present the results for the low frequency f=6.6 Hz. One observes that there are less stripes formed in the system compared with Fig. 5(a), and that the variation range of $N(w)$ is relatively small for all values of w, i.e. the initially formed patterns do not change much with time. Therefore, lowering of frequency slows down the underlying dynamics of the evolving patterns, reflected in the total number of stripes, in the coarsening behavior, and in the formation of layers (Fig. 3). At extremely low frequencies no pattern forms and the particles move with the surrounding fluid in a periodic manner. Figure 5(b) also shows that the dominant steady-state width shifts towards thicker stripes ($w_{\max} \sim 4d$) with decreasing f. Roughly speaking, the relaxation time of an object of size w in the fluid flow ($\sim w^2$ in low Reynolds number regime) tends to be synchronized with the characteristic time of the fluid motion ($\sim 1/f$) in the steady state, which results in $w \sim 1/\sqrt{f}$. However, in practice, the most probable width $w_{\max}$ increases slower with decreasing f.

IV. STEADY STATE

Next we investigate the probability distribution $P(w)$ of the stripe thickness to better understand the evolution of patterns. While the initial state of the patterns depends on the preparation conditions, after a short transient time t_s (of the order a few seconds), $P(w)$ starts to systematically evolve towards the steady state distribu-

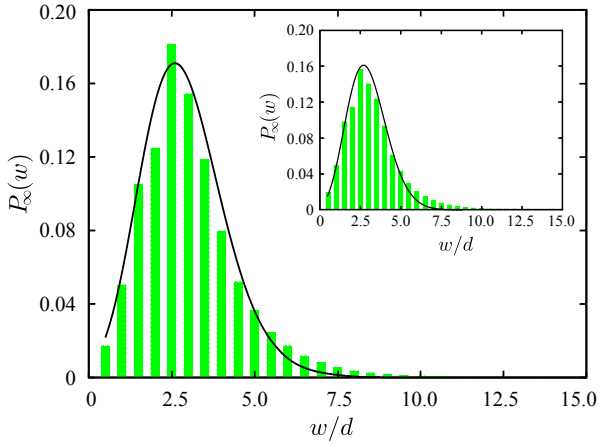

FIG. 7: $P_\infty(w)$ at f=19.8 Hz in the steady state (t=320s). The solid line denotes a fit by Eq. 2 with $\bar{w}$=2.8d. Inset: $P_\infty(w)$ at f=16.5 Hz.

tion $P_\infty(w)$: First, $P(w)$ becomes narrower while the peak position shifts towards wider stripes. Nevertheless, this process stops after a while, then, the peak position remains unchanged whereas $P(w)$ gets gradually broader and relaxes towards $P_\infty(w)$ (see Fig. 6).

Let us denote the mean number of particles on a horizontal plane and the mean number of stripes along the oscillation direction (i.e. the x-axis) by $\bar{n}_{\rm xy}$ and $\bar{N}$, respectively. Since both $\bar{n}_{\rm xy}$ [according to Fig. 3(a)] and $\bar{N}$ (not shown) reach a saturation value in the steady state, the mean number of particles on a 1D band parallel to the x-axis, $\bar{n}_{\rm x}$=$\bar{n}_{\rm xy}/(L_{\rm y}/d)$, and thus the average stripe-width $\bar{w}$=$\bar{n}_{\rm x}/\bar{N}$ converge to constant values as well. Assuming that, far from the initial conditions, the evolution of a stripe (including formation, coarsening, shrinkage, or dissolving) is a purely stochastic process, we consider the stripe width w as a random variable in the interval $[0, L_x]$ with the known average $\bar{w}$. One expects that under these conditions, the steady-state probability distribution of w can be approximated by the Poisson distribution:

$$P_\infty(w) = \frac{\bar{w}^w \exp(-\bar{w})}{w!}. \qquad (2)$$

A quantitative comparison between the above equation and the experimental data is presented in Fig. 7. The overall agreement is satisfactory, even though the tail of the experimental data decays slower than the Poisson function. We note that deviation of $P_\infty(w)$ from Eq. (2) occurs at low frequencies of oscillation. In the case of binary dry mixtures, a Gaussian distribution was reported for $P_\infty(w)$ whose mean depends on the occupied volume fraction [21].

V. SIMULATION RESULTS

To aid our understanding of the mechanism of the stripe formation, we perform molecular dynamics (MD) simulations, which has been previously employed to reproduce the experimental data [6, 16, 24]. We consider spherical soft particles with radii uniformly distributed between $0.95\bar{r}$ and $1.05\bar{r}$, which occupy a volume fraction of $\phi\simeq$0.11. The simulation box has dimensions $L_x\times L_y\times L_z$ (with L_x=$10^4\bar{r}$, L_y=$10^3\bar{r}$, and L_z=$10\bar{r}$) and is periodic in the x direction. The ratio between the particle and the fluid density is set to 0.96. The normal component of the interparticle interaction is given by a Hertzian repulsive force with viscous dissipation,

$$F_n = k\delta^{3/2} + \gamma_n \delta^{1/2}\dot{\delta}, \qquad (3)$$

where k, δ, and γ_n are the spring constant, normal overlap, and damping parameter, respectively. The particle-wall interaction is treated in the same way. k and γ_n depend on the elastic properties of the material and the radii of colliding particles (in practice, the average radius at low size polydispersity) [28]. The interaction in the tangential direction is modeled using the force law F_t=$\gamma_t|v_t^{\rm rel}|$, with γ_t and $v_t^{\rm rel}$ being the viscous damping and the relative surface velocity in the tangential direction, respectively. The Coulomb's criterion constrains the upper limit of F_t to $F_t^{\rm max}$=$\mu|F_n|$ (The data is shown for the friction coefficient μ=0.5). The fluid-particle interaction is modeled via an effective Stokes's drag force F_d proportional to the relative velocity $v_f^{\rm rel}$ between the particle and the fluid, F_d=$-\gamma_d v_f^{\rm rel}$ [16, 20, 24], where γ_d (obtained from the empirical equation of Ergun [29]) depends on viscosity and volume fraction. The influence of thermal fluctuations can be incorporated by adding a random noise to this equation (resulting in a Langevin-type dynamics) [30].

Using this model, we carry out simulations that are able to reproduce the observed behavior in experiments (see Fig. 8). The cell is vibrated sinusoidally with frequency f and amplitude A. The initial homogeneous state either remains well-mixed or quickly turns into a striped pattern, depending on the choice of the parameter values. Numerical simulations enable us to systematically determine the criteria under which the patterns form. For example, we find that the interparticle as well as wall-particle friction plays a crucial role in the formation of patterns. Indeed, no evidence for stripe formation was observed below $\mu\sim$0.1 in our simulations. Moreover, increasing the restitution coefficient of the collisions leads to nontrivial thickening of the stripes. The details of the extensive exploration of the parameter space for the pattern formation subdomain and their structural properties is beyond the scope of the present study and will be reported elsewhere. Here, we restrict the parameters to those of the experiments and focus on the structural characteristics of the resulting stripes. In contrast to the experiments, the initially formed distribution of the stripe width $P(w)$ at A=$5\bar{r}$ and f=20 Hz is a monotonically decreasing function of w which can be well fitted to an exponential decay [Fig. 8(a)]. The discrepancy can be attributed to the differences in the initial conditions and parameter values. The eventual

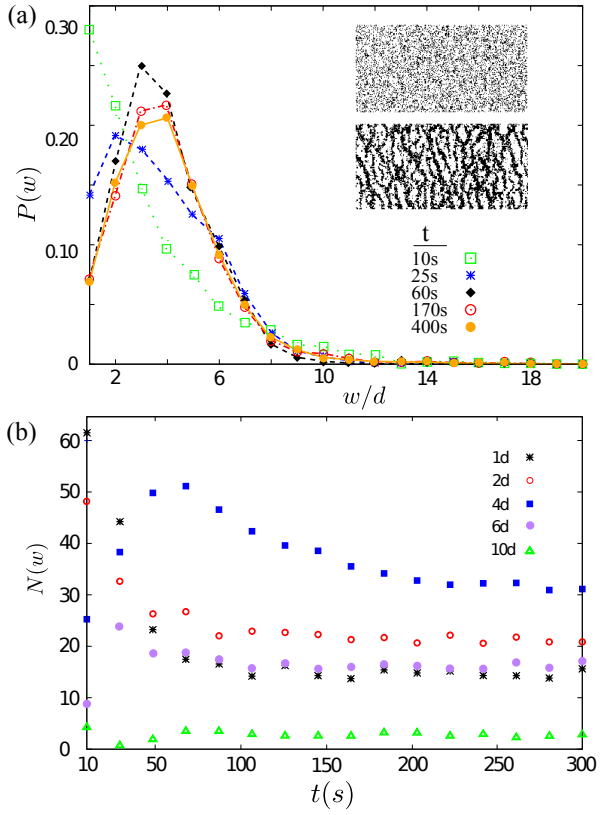

FIG. 8: (a) Evolution of the probability distribution $P(w)$ in MD simulations. Inset: Snapshots of particle positions, projected on the xy-plane, taken at t=5s (top) and t=300s (bottom). (b) The average width-resolved number of stripes $N(w)$ along the x-axis as a function of time.

form of $P(w)$, however, nearly follows a Poisson distribution with a peak at $w{\sim}4d\,(=8\bar{r})$. Noticeably, the evolution of the width-resolved number of stripes $N(w)$ is also satisfactorily reproduced [Fig. 8(b)]. As a final remark, we note that varying the strength of the random noise (in the Langevin-type variant of the model) does not affect the probability distribution $P(w)$ significantly, while it clearly changes the average persistence length of the stripes. For very high noise strengths, the oscillatory drive is unable to generate order and the system remains in the mixed state.

VI. CONCLUSION AND OUTLOOK

We have shown experimentally that the sinusoidal horizontal excitation of granular suspensions induces branched stripes aligned orthogonal to the direction of the periodic forcing. We characterized the structure by the probability distribution of the stripe thickness and verified that the structural changes evolve towards a dynamical saturation. It remains for further investigation to analyze the other structural features, such as spacefilling and branching properties; and also to clarify the role of key parameters on the formation and evolution of the patterns, aiming at understanding the underlying mechanisms and the possibility to design and control novel types of patterns.

Acknowledgments

We thank H. Parishani of the University of Delaware for helpful discussions and comments and H. Pacheco for help with the experiments. R.M. and M.M. acknowledge the financial support by the IASBS Research Council under grant No.G2008IASBS136.

[1] I. S. Aranson and L. S. Tsimring, Rev. Mod. Phys. **78**, 641 (2006).
[2] A. Kudrolli, Rep. Prog. Phys. **67**, 209 (2004).
[3] D. A. Sanders et al., Phys. Rev. Lett. **93**, 208002 (2004).
[4] C. Cattuto et al., Phys. Rev. Lett. **96**, 178001 (2006); M. R. Shaebani, J. Sarabadani, and D. E. Wolf, Phys. Rev. Lett. **108**, 198001 (2012).
[5] S. G. K. Tennakoon and R. P. Behringer, Phys. Rev. Lett. **81**, 794 (1998).
[6] D. Krengel et al., Granular Matter **15**, 377 (2013).
[7] E. Caglioti et al., Europhys. Lett. **43**, 591 (1998); G. Metcalfe et al., Phys. Rev. E **65**, 031302 (2002); T. Shinbrot and F. J. Muzzio, Phys. Rev. Lett. **81**, 4365 (1998).
[8] C. P. Clement et al., Europhys. Lett. **91**, 54001 (2010).
[9] M. E. Möbius et al., Nature **414**, 270 (2001); D. C. Hong, P. V. Quinn, and S. Luding, Phys. Rev. Lett. **86**, 3423 (2001); T. Shinbrot, Nature **429**, 352 (2004).
[10] D. A. Sanders et al., Europhys. Lett. **73**, 349 (2006); L. T. Lui et al., Phys. Rev. E **75**, 051303 (2007).
[11] C. Barentin, E. Azanza, and B. Pouligny, Europhys. Lett. **66**, 139 (2004).
[12] K. M. Hill and Y. Fan, Phys. Rev. Lett. **101**, 088001 (2008).
[13] D. Fenistein and M. van Hecke, Nature **425**, 256 (2003); R. Moosavi, M. R. Shaebani, M. Maleki, J. Török, D. E. Wolf, and W. Losert, Phys. Rev. Lett. **111**, 148301 (2013).
[14] S. Aumaitre, C. A. Kruelle, and I. Rehberg, Phys. Rev. E **64**, 041305 (2001); A. P. J. Breu, C. A. Kruelle, and I. Rehberg, Europhys. Lett. **62**, 491 (2003); T. Schnautz, R. Brito, C. A. Kruelle, and I. Rehberg, Phys. Rev. Lett. **95**, 028001 (2005).
[15] P. M. Reis et al., Europhys. Lett. **66**, 357 (2004).
[16] M. Pica Ciamarra, A. Coniglio, and M. Nicodemi, Phys. Rev. Lett. **94**, 188001 (2005).
[17] T. Mullin, Phys. Rev. Lett. **84**, 4741 (2000).
[18] C. M. Pooley and J. M. Yeomans, Phys. Rev. Lett. **93**, 118001 (2004).
[19] M. Fujii, A. Awazu, and H. Nishimori, Phys. Rev. E **85**, 041304 (2012).

[20] M. Pica Ciamarra, A. Coniglio, and M. Nicodemi, Phys. Rev. Lett. **97**, 038001 (2006).
[21] P. M. Reis and T. Mullin, Phys. Rev. Lett. **89**, 244301 (2002).
[22] G. C. M. A. Ehrhardt, A. Stephenson, and P. M. Reis, Phys. Rev. E **71**, 041301 (2005).
[23] P. M. Reis, T. Sykes, and T. Mullin, Phys. Rev. E **74**, 051306 (2006).
[24] P. Sánchez, M. R. Swift, and P. J. King, Phys. Rev. Lett. **93**, 184302 (2004).
[25] D. Klotsa et al., Phys. Rev. E **79**, 021302 (2009).
[26] M. Maleki, H. Pacheco, C. R. Suárez, and E. Clément, in *Traffic and Granular Flow'07*, edited by C. Appert-Rollan et al. (Berlin: Springer) 2009, pp. 621-627.
[27] D. Pihler-Puzović and T. Mullin, Proc. R. Soc. A **469**, 20130203 (2013).
[28] N. V. Brilliantov et al., Phys. Rev. E **53**, 5382 (1996).
[29] S. Ergun, Chem. Eng. Prog. **48**, 89 (1952).
[30] A. Wysocki and H. Löwen, Phys. Rev. E **79**, 041408 (2009); J. Phys. Condens. Matter **23**, 284117 (2011).